

IceCube as a Direct Detector of sub-GeV Dark Matter

**Allegra Cavicchi,^{a,*} Gwenhaël W. de Wasseige,^b Mathieu Lamoureux,^b
Jonathan Mauro^b and Filippo Sala^a**

^a*Dipartimento di Fisica e Astronomia "Augusto Righi",
Università di Bologna, via Irnerio 46, Bologna, Italy*

^b*Centre for Cosmology, Particle Physics and Phenomenology - CP3,
Université Catholique de Louvain, B-1348 Louvain-la-Neuve, Belgium*

*E-mail: allegra.cavicchi@studio.unibo.it,
gwenhael.dewasseige@uclouvain.be, mathieu.lamoureux@uclouvain.be,
jonathan.mauro@uclouvain.be, f.sala@unibo.it*

The study of non-gravitational effects of Dark Matter (DM) is a growing field of research, leading to the development of numerous dedicated experiments. Astrophysical and cosmological observations show that the galactic component of DM is non-relativistic; this results in a rapid loss of sensitivity to sub-GeV DM masses in Direct Detection experiments with nuclear targets sensitive to keV-scale recoil energies.

Relying only on the assumption that DM scatters on a Standard Model (SM) target particle, a higher-speed component of the flux arises, originating from the upscattering of the galactic DM by Cosmic Rays, which peaks in the GeV energy range. Neutrino telescopes like Super-Kamiokande are sensitive to these energies and have already been used as DM detectors, setting world-leading limits. Higher energy telescopes, such as IceCube, are also sensitive to these energies and could be even more promising, given their larger volumes. How to best use them to detect sub-GeV DM?

In this contribution, we will address this question for both spin-independent and spin-dependent DM-SM interactions and estimate the sensitivity of IceCube to the scatterings of sub-GeV DM with nuclei.

39th International Cosmic Ray Conference (ICRC2025)
15–24 July 2025
Geneva, Switzerland



*Speaker

1. Introduction

In the past decades, astrophysical and cosmological observations have established the existence of a new form of matter, different from ordinary matter, which is not luminous and is therefore known as "dark matter" (DM). Its existence has been known up to now only from its gravitational effects, while all its other potential interactions are beyond our current knowledge. Thus, the study of DM non-gravitational impacts is a growing field of research, leading to numerous specialized experiments, see [1] for a recent review.

Among these experiments, the Direct Detection (DD) ones attempt to observe the DM scattering on a SM particle, observed through the target recoil energy reconstruction. Astrophysical and cosmological data tell us that the galactic component of DM is non-relativistic ($v \sim 10^{-3}$ within the Milky Way halo); therefore, sub-GeV DM induces nuclear recoil energies below $O(\text{keV})$. The largest existing DD experiments, which are sensitive to keV-scale recoil energies, become then insensitive to sub-GeV DM masses very rapidly.

New experimental techniques have been proposed to be sensitive to the low recoil energies induced by halo DM, see e.g. [2]. Another possibility for direct detection of sub-GeV DM is to rely on its high-energy fluxes that are necessarily generated if DM interacts with the SM, for example, from cosmic ray (CR) upscattering [3, 4]. This makes their search optimal at neutrino detectors, as proven, e.g., by Super-Kamiokande [5]. Are even larger neutrino detectors sensitive to sub-GeV DM?

In particular, IceCube, a neutrino telescope located near the Amundsen-Scott South Pole Station, is the first gigaton-scale, cubic-kilometer neutrino detector ever built and the largest operating one. Although it was primarily designed to observe neutrinos from the most violent astrophysical sources in our universe, it can also be a powerful tool for DM searches, given the extremely weak interaction strength of DM, comparable to that of neutrinos.

IceCube has already been used for DM indirect searches [6], which aim to detect SM particles produced by DM decays or annihilations outside the detector. In this study, we begin the exploration of the extent it can be used for DM DD. In particular, we investigate IceCube sensitivity as a Direct Detector of CR-upscattered sub-GeV Dark Matter, in the assumption that DM particles can interact with SM quarks. A more detailed development of the framework, methodology, and analysis method explored in this work can be found in [7].

2. Theoretical Framework

In this study, we define the DM candidate as a Dirac fermion χ , singlet under the Standard Model (SM) gauge group, with mass m_χ . We will be interested in DM relativistic scatterings, both with CRs and in ice. Therefore we need to go beyond the constant cross-section parametrization for DM-SM interactions. We then add to the SM matter content, in addition to the DM fermion, a new particle that mediates its interaction with SM particles. We consider two cases: a new scalar mediator ϕ with mass m_ϕ , and a new pseudoscalar mediator a with mass m_a , that mediate DM-hadron interactions via the following Lagrangians ($q = u, d$) [8]:

$$\begin{aligned}\mathcal{L}_\phi &= g_{\chi\phi}\bar{\chi}\chi\phi + g_{q\phi}\bar{q}q\phi, \\ \mathcal{L}_a &= g_{\chi a}\bar{\chi}i\gamma_5\chi a + g_{qa}\bar{q}i\gamma_5qa.\end{aligned}\tag{1}$$

The non-relativistic operators for nucleus scattering in momentum space, induced by \mathcal{L}_ϕ and \mathcal{L}_a , are [9], respectively,

$$\mathcal{L}_{N\phi} : \mathbb{1}, \quad \mathcal{L}_{Na} : (\vec{s}_\chi \cdot \vec{p})(\vec{s}_N \cdot \vec{p}), \quad (2)$$

where \vec{s}_N is the nucleus spin, \vec{s}_χ the DM one, and \vec{q} is the momentum exchanged in the DM-nucleon ($\chi - N$) scattering. Hence, in the non-relativistic limit relevant for DD of halo DM, \mathcal{L}_ϕ induces spin-independent interactions, while \mathcal{L}_a spin- and momentum-suppressed ones. For both DM scatterings, both with CRs and in ice, we need the differential cross sections for DM elastic scatterings with nuclei and nucleons. For each mediator, those with nucleons read

$$\begin{aligned} \frac{d\sigma_\phi}{dK_f} &= \frac{1}{K_{\max}} \frac{g_{\chi\phi}^2 g_{N\phi}^2}{16\pi s} \frac{(4m_\chi^2 - t)(4m_N^2 - t)}{(t - m_\phi^2)^2} F_N^2(-t) \Theta(K_{\max} - K_f), \\ \frac{d\sigma_a}{dK_f} &= \frac{1}{K_{\max}} \frac{g_{\chi a}^2 g_{Na}^2}{16\pi s} \frac{t^2}{(m_a^2 - t)^2} F_a^2(-t) \Theta(K_{\max} - K_f), \end{aligned} \quad (3)$$

where s, t are the Mandelstam variables, $g_{N\phi, Na}$ are functions of $g_{q\phi, qa}$, K_{\max} is the maximum transferred kinetic energy, and $F_{A,a}(q^2) = (1 + \frac{q^2}{\Lambda_{A,a}^2})^{-1}$ are the form factors, see [8] for more details.

2.1 Dark Matter upscattered flux

In DM-CRs interactions, where the DM particles are initially at rest while CRs are relativistic, DM particles can acquire a fraction of the CRs' kinetic energy and become this way more energetic than halo DM. The upscattered component of the DM flux can then scatter with target particles in our detectors on Earth. These scatterings can be measured because CR-upscattered DM releases more energy than halo one, so that the target recoil energy can exceed the experimental threshold.

As customary, we assume a CR flux homogeneous in a leaky cylinder centered on the galactic center, and vanishing outside. Therefore, the DM flux upscattered by the CRs is given by

$$\frac{d\Phi_\chi}{d\Omega} = \frac{J(l, b)}{m_\chi} \sum_A \int dK_A \frac{d\Phi_A}{d\Omega} \frac{d\sigma}{dK_\chi}, \quad (4)$$

where $J(b, l)$ is the J -factor, K_A is the CRs kinetic energy, $d\sigma/dK_\chi$ is the cross-section discussed above, and $d\phi_A/d\Omega$ is the differential CRs flux, which has been extracted from Ref. [10].

In practice, $A = p, \text{He}$ for the scalar mediator case, while $A = p$ for the pseudoscalar one, because helium does not have net spin.

The J -factor is an astrophysical quantity, which depends on l and b , respectively the galactic longitude and latitude, and embeds the DM- and CR-distributions in the galaxy. We define it as

$$J(b, l) = \int_{l.o.s} dL \rho_\chi(r) = \int_{l.o.s} dL \rho_\odot \frac{r_\odot(r_\odot + r_c)^2}{r(r + r_c)^2}, \quad (5)$$

since we consider the Navarro–Frenk–White (NFW) DM density profile $\rho_\chi(r) = \rho_{\text{NFW}}(r)$ [11], with $r_\odot = 8.5$ kpc, $r_c = 20$ kpc, $\rho_\odot = 0.42$ GeV/cm³. We expect the majority of our DM signal in correspondence of the Galactic Center, i.e. around $(l, b) = (0^\circ, 0^\circ)$. This is an essential feature of our signal, which can be considered in our analysis.

In Figure 1 we report the sky-integrated DM fluxes computed for the scalar and pseudoscalar mediator case. As a comparison, we also report the Halo DM flux. Even if the upscattered DM

fluxes are less intense than the halo one, they are peaked at much higher energies, of the order of the GeV. This is a crucial feature to enable DM DD for neutrino experiments, because they are sensitive to these energies.

2.2 Flux attenuation

Since the IceCube Neutrino Telescope is located in the Antarctic Ice, at a depth between 1450 m and 2450 m, the DM particles have to travel a given amount of ice (or both ice and Earth's rocks, depending on their incoming direction) before reaching the detector. Therefore, we have to consider that DM can scatter on ice or Earth's rocks while traveling to reach the detector, resulting in an attenuation of the DM flux.

What encodes this attenuation is the DM kinetic energy \bar{K}_χ at the depth z , which is smaller with respect to the non-attenuated kinetic energy K_χ . We can define this attenuation considering the following differential equation [12]:

$$\frac{d\bar{K}_\chi(z)}{dz} = \sum_T n_T \int dK_T K_T \frac{d\sigma}{dK_T}, \quad (6)$$

where n_T is the number density of a target particle inside the crossed material; in our case these number densities are obtained by the mass densities $\rho_{p+n}^{\text{Earth}} = 2.7 \text{ g/cm}^3$ and $\rho_{p+n}^{\text{Ice}} = 0.92 \text{ g/cm}^3$. The depth z travelled inside matter depends on the incoming direction of the DM particle.

In this study, we have chosen to consider only the component coming from the galactic center for the attenuated flux, since the NFW distribution is strongly peaked in it¹. The distance traveled by particles coming from this direction is approximately $z = 5.16 \text{ km}$, and this path is all inside Antarctic ice; therefore, the attenuation of the DM flux coming from the Galactic Center is only due to ice.

2.3 Number of Expected Events at the detector

We can start from the previous knowledge about neutrino-proton interaction in IceCube and, determining the corrections needed, we can study the DM interactions in the detector. To be sensitive to an energy range of $E_\chi > 500 \text{ MeV}$, we consider a combination of IceCube's *ELOWEN* and *GRECO* event selections.

The differential number of expected DM events in the detector is given by

$$\frac{dN_\chi}{d\Omega}(l, b) = t \int dK_\chi \frac{d\Phi_\chi}{d\Omega}(K_\chi l, b) A_{\text{eff}}^\chi(K_\chi). \quad (7)$$

where t is the acquisition time, A_{eff}^χ is the DM effective area, and $\frac{d\Phi_\chi}{d\Omega}(K_\chi, l, b)$ is the differential DM flux. The DM effective area is obtained by rescaling the neutrino effective area by the ratio of the DM-proton cross section with the neutrino-proton cross section such that $A_{\text{eff}}^\chi(K_\chi) = \frac{\sigma_{\chi p}(K_\chi)}{\sigma_{\nu p}(K_\nu)} A_{\text{eff}}^\nu(K_\nu)$.

Since *ELOWEN* and *GRECO* public effective areas are the total ones, we have considered the total neutrino cross section to rescale them and obtain the DM effective area. The use of the neutral

¹This approximation was introduced to improve the code's efficiency. Nevertheless, we have also implemented the full analytical computation of the attenuated number of events, which converges to the approximate result in the direction of the Galactic Center.

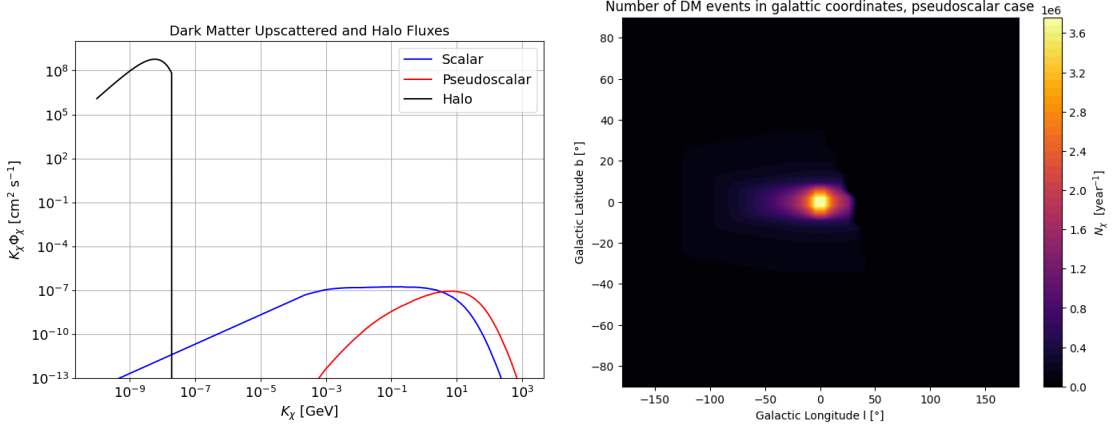


Figure 1: Left: DM fluxes at Earth for scalar (in blue) and pseudoscalar (in red) mediator, for the following values of the parameters: $m_\chi = 10$ MeV, $m_\phi = m_a = 1$ GeV and $g_\chi \phi g_{u\phi} = g_\chi \phi g_{d\phi} = g_\chi a g_{ua} = g_\chi a g_{da} = 0.1$. The Halo component (in black) is also shown as a comparison. Right: Number of expected events as a function of the galactic coordinates for *GRECO* event selection; this plot has been computed for the pseudoscalar mediator case, with fixed parameters $m_\chi = 10$ MeV, $m_a = 1$ GeV and $g_\chi a g_{ua} = g_\chi a g_{da} = 0.1$. The asymmetry respect to the GC is given by the cut on $\delta \leq -5^\circ$ of $A_{\text{eff}}^{\nu, \text{GRECO}}$.

current $A_{\text{eff}}^{\nu, \text{NC}}$ (if available) and $\sigma_{\nu p}^{\text{NC}}$ would be more correct, because the final state would be an upscattered proton as for the DM case. Our procedure of using the neutral plus charged current ones still provides a reasonable approximation if the energy shape is the same between $\sigma_{\nu p}^{\text{NC}}$ and $\sigma_{\nu p}$ (which it is), as well as between $A_{\text{eff}}^{\nu, \text{NC}}$ and A_{eff}^ν .

Another aspect that can be considered in this analysis is the directionality of the signal. The *ELOWEN* event selection does not provide direction-reconstruction [13], therefore the sky-integrated number of expected events is used:

$$N_\chi^{\text{ELOWEN}} = \int_{-\pi}^{\pi} dl \int_{-\pi/2}^{\pi/2} db \sin b \frac{dN_\chi}{d\Omega}(l, b). \quad (8)$$

On the other hand, the *GRECO* event selection is sensitive to the sky direction. We can therefore use the public effective areas [14] in the declination band $\delta \in [-90^\circ, -5^\circ]$, which is where the galactic center lies and the majority of the DM flux is expected. The total number of events for *GRECO* event selection becomes

$$\frac{dN_\chi^{\text{GRECO}}}{d\Omega}(\alpha, \delta) = \int_{-\pi}^{\pi} d\alpha \int_{-90^\circ}^{-5^\circ} d\delta \sin \delta \frac{dN_\chi}{d\Omega}(\alpha, \delta). \quad (9)$$

This number can be converted to $dN_\chi^{\text{GRECO}}(l, b)/d\Omega$ by a simple change of coordinates. We then define a binning of 9×9 (81 bins) in galactic longitude and latitude.

In Figure 1, an example of the differential number of DM events, obtained considering *GRECO* effective area, is shown.

Finally, in Figure 2 we present, as a reference, the 2D histograms in the galactic coordinates for the *GRECO* background and signal for the pseudoscalar mediator case.

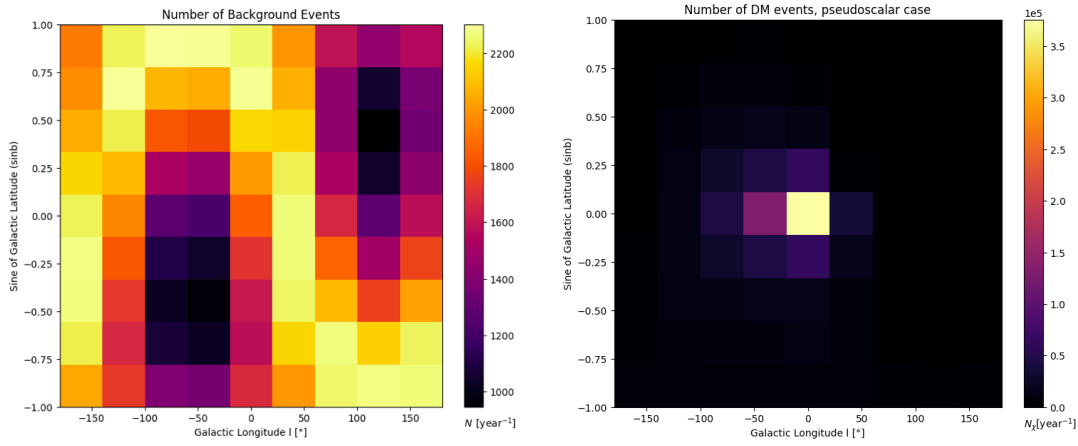


Figure 2: Left: *GRECO* background in the galactic coordinates; it is evident that is peaked at the horizon and minimum at the poles. Right: *GRECO* expected signal for the pseudoscalar mediator case with $m_\chi = 0.01$ GeV, $m_a = 1$ GeV, $g_{ua}g_{\chi a} = g_{da}g_{\chi a} = 0.1$.

3. New IceCube Sensitivities to sub-GeV Dark Matter

Given the number of expected events from the two event selections, we can perform a **binned likelihood analysis** of the number of events as a function of the DM mass and of the coupling; we consider 9 bins in both galactic coordinates and therefore we obtain 81 signal values for the *GRECO* case, to which one sky-integrated signal value for *ELOWEN* is added.

Assuming that *ELOWEN* and *GRECO* are independent samples (which is a reasonable assumption since they are two independent event selections), the likelihood \mathcal{L} can be defined² as

$$\mathcal{L}(\{N_i\}|\{B_i\}, m_\chi, g) = \prod_{i=1}^{82} \text{Poisson}(N_i, B_i + S_i(m_\chi, g)). \quad (10)$$

where the product runs over the 81 bins for *GRECO* and the *ELOWEN* sky-integrated observation.

Finally, to confront the null hypothesis (background-only hypothesis) with our model (signal + background hypothesis), we consider the minus log-likelihood test statistic

$$\text{TS}(m_\chi, g) = 2 \ln \frac{\mathcal{L}(N_j|\hat{m}_j, \hat{g}_j, \hat{B}_e)}{\mathcal{L}(N_j|m_\chi, g=0, B_e)}, \quad (11)$$

where $\hat{m}_j, \hat{g}, \hat{B}_e$ are the parameters which maximize the likelihood, while $\mathcal{L}(N_j|m_\chi, g=0, B_e)$ corresponds to the background only hypothesis, since in our model $g=0$ means signal absence.

In the minimization, the *ELOWEN* background is a free parameter since it cannot be assumed that the measured event rate is independent of our signal, on the contrary, this is possible in *GRECO* due to the direction reconstruction of the events.

We draw one thousand pseudo-experiments to obtain the TS distributions for the background-only hypothesis, imposing $N_j = B_j$. Similarly, we can derive the signal-plus-background distribution for each DM mass and coupling, imposing $N_j(m_\chi, g) = B_j + S_j(m_\chi, g)$. Finally, to obtain the

²In the following, we refer to the product of the couplings, for both scalar and pseudoscalar case, as $g = g_{u\phi}g_{\chi\phi} = g_{ua}g_{\chi a}$

90% sensitivity contours in the (m_χ, g) plane, we compute all the (m_χ, g) pairs for which 90% of the signal TS distribution is above the median of the background TS distribution.

These contour plots are shown, for the scalar and pseudoscalar case, in Figures 3 and 4, respectively.

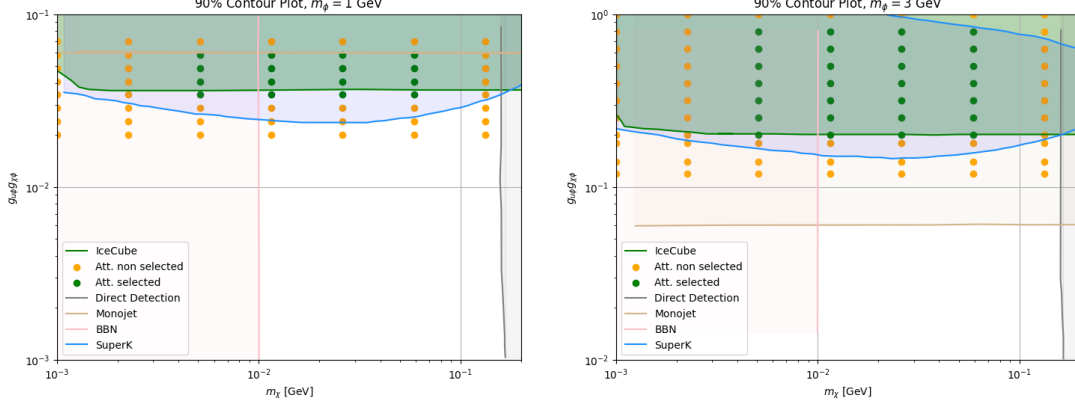


Figure 3: 90% Contour plot in the plane of couplings vs DM mass, for the scalar mediator of mass $m_\phi = 1$ GeV (left) and $m_\phi = 3$ GeV (right). With the green line, we represent the IceCube’s sensitivity, neglecting Earth and Ice attenuation. The effect of the latter is encoded in the points, where the green ones indicate the parameter space where IceCube is still sensitive after including Ice attenuation.

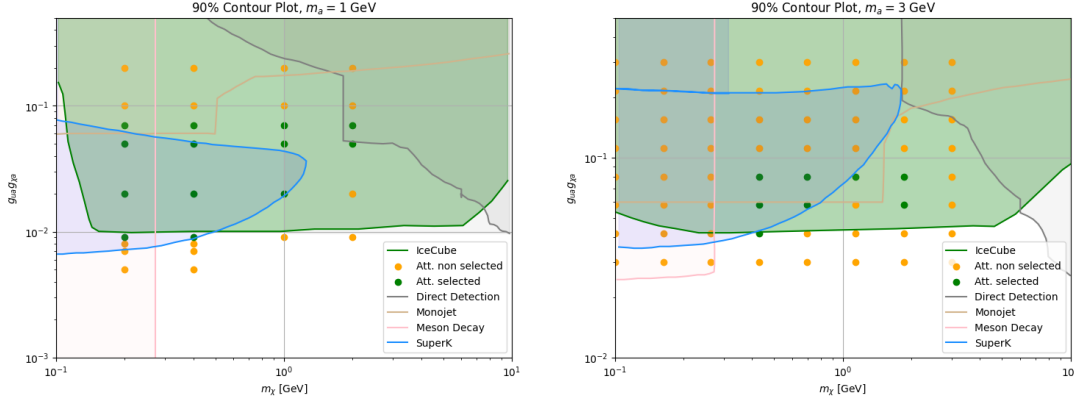


Figure 4: 90% Contour plot in the plane of couplings vs DM mass, for the pseudoscalar mediator of mass $m_a = 1$ GeV (left) and $m_a = 3$ GeV (right). Green line and shadings and points as in Fig. 3.

The preliminary IceCube’s sensitivity, obtained neglecting ice attenuation, is represented in green lines; furthermore, with green and orange dots are represented, respectively, the selected and non-selected points considering also ice attenuation, for which we have not drawn a contour since we need a better determination of the attenuated flux. Finally, for comparison, we also show Super-Kamiokande sensitivity (in light blue), and other limits known from the literature [8].

4. Conclusions and prospects

As shown in the contour plots (Figures 3 and 4), IceCube sensitivities are close to existing constraints by Super-Kamiokande. This gives encouraging prospects for continuing this study

with a more detailed analysis. Furthermore, even if the flux's attenuation has not been completely implemented yet, from our simple approximation we obtain hints that the behavior is consistent with the expectations: regions of the parameter spaces with high couplings (of the order of $g \sim 10^{-1}$) are not included in the contour plot, since the expected flux at the detector is strongly attenuated and therefore becomes indistinguishable from the background. In conclusion, this study presents the first investigation into using IceCube as a Dark Matter direct detector. Future analysis can benefit from a complete treatment of attenuations effects to the Dark Matter flux from the full galaxy. Further improvements can be obtained through a more detailed characterization of the low energy background, improving the *ELOWEN* contribution to the overall sensitivity.

Acknowledgements

The authors thank the IceCube collaboration for fruitful discussion. Computational resources have been provided by the supercomputing facilities of the Université catholique de Louvain (CISM/UCL) and the Consortium des Équipements de Calcul Intensif en Fédération Wallonie Bruxelles (CÉCI) funded by the Fond de la Recherche Scientifique de Belgique (F.R.S.-FNRS) under convention 2.5020.11 and by the Walloon Region. J.M. is a PhD fellow of FRiA du Fonds de la Recherche Scientifique - FNRS, M.L. is a Postdoctoral Researcher of the Fonds de la Recherche Scientifique - FNRS.

References

- [1] Marco Cirelli, Alessandro Strumia, and Jure Zupan. “Dark Matter”. In: (2024). arXiv: [2406.01705v2](#).
- [2] Essig, Rouven, et al. “Snowmass2021 Cosmic Frontier: The landscape of low-threshold dark matter direct detection in the next decade”. In: *Snowmass 2021*, Mar. 2022. arXiv: [2203.08297 \[hep-ph\]](#).
- [3] Bringmann, Torsten, and Pospelov Maxim. “Novel direct detection constraints on light dark matter”. In: *Phys. Rev. Lett.* **122**.17 (2019), p. 171801. arXiv: [1810.10543 \[hep-ph\]](#).
- [4] Yohei Ema, Filippo Sala, and Ryosuke Sato. “Light Dark Matter at Neutrino Experiments”. In: *Phys. Rev. Lett.* **122**.18 (2019), p. 181802. doi: [10.1103/PhysRevLett.122.181802](#). arXiv: [1811.00520 \[hep-ph\]](#).
- [5] K. Abe et al. “Search for Cosmic-Ray Boosted Sub-GeV Dark Matter Using Recoil Protons at Super-Kamiokande”. In: *Phys. Rev. Lett.* **130**.3 (2023), p. 031802. arXiv: [2209.14968 \[hep-ex\]](#).
- [6] IceCube Collaboration. “Search for dark matter from the center of the Earth with ten years of IceCube data”. In: (2024). arXiv: [2412.12972v1](#).
- [7] Allegra Cavicchi. “Cosmic-ray upscattered dark matter and its searches with IceCube”. MA thesis. University of Bologna, 2025. URL: <https://amslaurea.unibo.it/id/eprint/35877/>.
- [8] Yohei Ema, Filippo Sala, and Ryosuke Sato. “Neutrino experiments probe hadrophilic light dark matter”. In: *SciPost Phys.* **10**, 072 (2020). arXiv: [2011.01939v2](#).
- [9] JiJi Fan, Matthew Reece, and Lian-Tao Wang. “Non-relativistic effective theory of dark matter direct detection”. In: *JCAP* **1011**:042 (2010). arXiv: [1008.1591v2](#).
- [10] Ethan Silver and Elena Orlando. “Testing Cosmic-Ray Propagation Scenarios with AMS-02 and Voyager Data”. In: (2024). arXiv: [2401.06242](#).
- [11] Julio F. Navarro, Carlos S. Frenk, and Simon D.M. White. “The Structure of Cold Dark Matter Halos”. In: *Astrophys.J.* **462**:563-575 (1995). arXiv: [astro-ph/9508025v1](#).
- [12] Timon Emken and Chris Kouvaris. “How blind are underground and surface detectors to strongly interacting dark matter?” In: *Phys. Rev. D* **97**, 115047 (2018). arXiv: [1802.04764v2](#).
- [13] The IceCube Collaboration. “Limits on Neutrino Emission from GRB 221009A from MeV to PeV using the IceCube Neutrino Observatory”. In: *ApJL* **946** L26 (2024). arXiv: [2302.05459v3](#).
- [14] The IceCube Collaboration. “Search for sub-TeV Neutrino Emission from Novae with IceCube-DeepCore”. In: *ApJ* **953** 160 (2023). arXiv: [2212.06810v4](#).